

## Breakdown of QCD factorization at large Feynman $x$

B. Z. Kopeliovich,<sup>1,2</sup> J. Nemchik,<sup>3</sup> I. K. Potashnikova,<sup>1,2</sup> M. B. Johnson,<sup>4</sup> and Ivan Schmidt<sup>1</sup>

<sup>1</sup>*Departamento de Física, Universidad Tecnica Santa Maria, Valparaiso, Chile*

<sup>2</sup>*Max-Planck Institut für Kernphysik, Heidelberg, Germany*

<sup>3</sup>*Institute of Experimental Physics SAV, Kosice, Slovakia*

<sup>4</sup>*Los Alamos National Laboratory, Los Alamos, New Mexico 87545, USA*

(Received 17 February 2005; published 23 November 2005)

Recent measurements by the BRAHMS Collaboration of high- $p_T$  hadron production at forward rapidities at the BNL Relativistic Heavy Ion Collider found the relative production rate  $(d\text{-Au})/(p\text{-p})$  to be suppressed rather than enhanced. Examining other known reactions (forward production of light hadrons, the Drell-Yan process, heavy flavor production, etc.), one notes that all of these display a similar property, namely, their cross sections in nuclei are suppressed at large  $x_F$ . Since this is the region where  $x_2$  is minimal, it is tempting to interpret this as a manifestation of coherence or of a color glass condensate, whereas it is actually a simple consequence of energy conservation and takes place even at low energies. We demonstrate that in all these reactions there is a common suppression mechanism that can be viewed, alternatively, as a consequence of a reduced survival probability for large rapidity gap processes in nuclei, a Sudakov suppression, an enhanced resolution of higher Fock states by nuclei, or an effective energy loss that rises linearly with energy. Our calculations agree with the data.

DOI: [10.1103/PhysRevC.72.054606](https://doi.org/10.1103/PhysRevC.72.054606)

PACS number(s): 24.85.+p, 13.85.-t, 25.40.Ve, 25.80.Ls

### I. INTRODUCTION

It is believed that in order to reach the smallest values of the light-front momentum fraction variable  $x$  in nuclei, and thus access the strongest coherence effects such as those associated with shadowing or the color glass condensate, one should go to forward rapidities, i.e., to the beam fragmentation region at large Feynman  $x_F$ . This probably was the idea behind the measurements of high- $p_T$  hadron production in deuteron-gold collisions at large rapidities performed recently by the BRAHMS Collaboration [1] at the BNL Relativistic Heavy Ion Collider.

This proposition is based upon the usual leading-order relation between  $x_1$  and  $x_2$  for two colliding partons,  $x_1 x_2 = \hat{s}/s$ , where  $\hat{s}$  and  $s$  are the square of the c.m. energies of the colliding partons and hadrons, respectively. It is demonstrated in Sec. II, however, that although formally  $x_2$  reaches its minimal values as  $x_1 \rightarrow 1$ , the coherence phenomena vanish in this limit [2].

Moreover, it is shown in Sec. III that another effect causing considerable nuclear suppression for any reaction at large  $x_F$  can be easily misinterpreted as coherence. The source of this suppression may be understood in terms of the Sudakov form factor, which is the probability that no particles be produced as  $x_F \rightarrow 1$ , as demanded by energy conservation. Clearly, multiple interactions make it more difficult to satisfy this condition and therefore should cause an even greater suppression.

Spectator partons, both soft and hard, may also interact while propagating through the nucleus and populate the large rapidity gap (LRG) that forms when  $x_F \rightarrow 1$ . As long as production within the LRG is forbidden, the presence of spectators further reduces the survival probability of LRG processes [3].

This mechanism of suppression can also be understood in terms of the Fock-state decomposition of the nucleus. The

dominant Fock components are determined by the resolution of the interaction, and a nucleus can resolve more Fock states than a proton since the saturation scale  $Q_s$  rises with  $A$ . Thus, one can see that the leading parton distribution involves higher multiparton Fock states in a nucleus and must fall more steeply toward  $x_F = 1$ , as suggested by the Blankenbecler-Brodsky counting rule [4] (see also [5,6]).

Note that this situation is analogous to what happens when one of the bound nucleons in a relativistic nucleus is moving with a momentum higher than the average momentum of an individual nucleon. This is the mechanism of production of particles with  $x_F > 1$  in nuclear collisions [6].

The involvement of higher Fock states means that gluon bremsstrahlung is more intense in the interaction on a nucleus than on a proton target, i.e., it leads to larger energy loss. Because of this, the large  $x_F$  suppression may be envisioned to be a consequence of induced energy loss. Remarkably, such an induced energy loss proportional to energy results in  $x_F$  scaling. This is different from the energy-independent mean rate of energy loss found in [7–9]. The latter, however, was calculated with no restriction on the gluon radiation spectrum, a procedure that is not appropriate when  $x_F \rightarrow 1$  [10,11].

The nuclear effects under discussion violate QCD factorization. This happens because any hard reaction that is a LRG process in the limit  $x_F \rightarrow 1$ , e.g., gluon radiation, is forbidden by energy conservation throughout a rather large rapidity interval. On the other hand, factorization relates this process to the parton distribution functions measured in other reactions, for instance, deep-inelastic scattering (DIS), which do not have such a restriction.<sup>1</sup> The light-cone dipole description employed here does not involve a twist decomposition, but apparently

<sup>1</sup>See for example J. Qiu and I. Vitev, hep-ph/0405068, where the suppression of single-inclusive hadron production is described by power corrections that vanish for large transverse momentum.

the lack of factorization does not disappear with increasing scale. This will be confirmed below by explicit calculations for different hard reactions.

Thus, we conclude that the nuclear suppression imposed by energy conservation as  $x_F \rightarrow 1$  is a leading twist effect, breaking QCD factorization. This is at variance with the conclusion of [12], made on the basis of observed violation of  $x_2$  scaling in  $J/\Psi$  production off nuclei and assuming validity of the factorization theorem [13] even in the limit  $x_F \rightarrow 1$ .

Note that factorization is broken even for reactions on a free proton. For instance, the Drell-Yan reaction, which is a LRG process as  $x_F \rightarrow 1$ , cannot be expressed in terms of hadronic structure functions measured in deep-inelastic scattering.

## II. DISAPPEARANCE OF NUCLEAR SHADOWING AT SMALLEST $x_2$

It is convenient to study shadowing and other coherence effects in the rest frame of the nucleus. In this frame, the parameter controlling the interference between amplitudes of the hard reaction occurring on different nucleons is the longitudinal momentum transfer  $q_L$  related to the coherence length  $l_c = 1/q_L$ . The condition for the appearance of shadowing in a hard reaction is the presence of a coherence length that is long compared to the nuclear radius,  $l_c \gtrsim R_A$ .

Clearly at large  $x_1 \sim 1$ , a hard reaction is mediated by a projectile valence quark and looks like a hard excitation of the valence quark in this reference frame. For instance, the Drell-Yan (DY) process looks like radiation of a heavy photon/dilepton by a valence quark [14]. The coherence length in this case is related to the mean lifetime of a fluctuation  $q \rightarrow q\bar{l}$  and reads [2,14]

$$l_c = \frac{2E_q \alpha(1-\alpha)}{k_T^2 + (1-\alpha)M_{\bar{l}l}^2 + \alpha^2 m_q^2}. \quad (1)$$

Here  $\vec{k}_T$  and  $\alpha$  are the transverse momentum and the fraction of the light-cone momentum of the quark carried by the dilepton;  $M_{\bar{l}l}$  is the effective mass of the dilepton; and  $E_q = x_q s/2m_N$  and  $m_q$  are the energy and mass of the projectile valence quark. This simple kinematic formula reflects the relation between the longitudinal momentum transfer  $q_L = (M_{\bar{l}l}^2 - m_q^2)/2E_q$  and the coherence length  $l_c = 1/q_L$ . Note that the fraction of the proton momentum  $x_q$  carried by the valence quark in this reference frame is not equal to  $x_1$ , but  $\alpha x_q = x_1$ . Clearly, when  $x_1 \rightarrow 1$ , also  $\alpha \rightarrow 1$ , i.e., the coherence length Eq. (1) vanishes in this limit, and no shadowing is possible.

The onset of shadowing as a function of rising coherence length can be approximated with good accuracy as,

$$R_{A/N}^{\text{shad}} \approx 1 - \frac{1}{4} \sigma_{\text{eff}} \langle T \rangle F_A^2(q_L), \quad (2)$$

where  $R_{A/N}$  is the normalized ratio of the reaction rates on nuclear and nucleon targets.  $F_A(q_c)$  may be called the longitudinal nuclear form factor, defined as

$$F_A^2(q_L) = \frac{1}{\langle T_A \rangle} \int d^2b \left| \int_{-\infty}^{\infty} dz e^{iz/l_c} \rho_A(b, z) \right|^2, \quad (3)$$

where  $\langle T_A \rangle = 1/A \int d^2b T_A^2(b)$  is the nuclear thickness  $T_A(b)$  averaged over impact parameter  $b$  and is evaluated as the

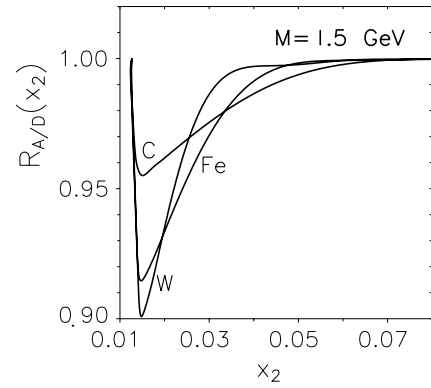


FIG. 1. Shadowing in DY reaction on carbon, iron, and tungsten as function of  $x_2$  at  $M_{\bar{l}l} = 4.5 \text{ GeV}$  and  $s = 1600 \text{ GeV}^2$ . Nuclear shadowing disappears both at large and small  $x_2$ , since the coherence length, Eq. (1), vanishes in both limits.

integral of the nuclear density over the longitudinal coordinate,  $T_A(b) = \int dz \rho_A(b, z)$ . The effective cross section

$$\sigma_{\text{eff}}(x_1, x_2, s) = \frac{\langle \sigma_{\bar{q}q}^2(\alpha r_T) \rangle}{\langle \sigma_{\bar{q}q}(\alpha r_T) \rangle} \quad (4)$$

was evaluated in [2].

With the mean value of  $l_c$  given by Eq. (3), the nucleus-to-deuteron ratios of DY cross sections are presented for different nuclei in Fig. 1 [2].

As expected, in accordance with Eq. (1), shadowing vanishes at the smallest value of  $x_2$  that can be accessed in DY reactions; while according to QCD factorization, it is expected to reach maximal strength.

Note that the shrinkage of the coherence length toward  $x_F = 1$  not only leads to the disappearance of shadowing in this kinematic limit but also reduces shadowing in DY compared to DIS throughout the entire range of  $x_2$ .

Note that the coherence length Eq. (1) linearly rises with energy; therefore, the interval of  $x_1$ , where the coherence length contracts down to the nuclear size, shrinks like  $1/E$  (see Sec. V D).

## III. SUDAKOV SUPPRESSION, OR SURVIVAL PROBABILITY OF LARGE RAPIDITY GAPS

The BRAHMS experiment [1] found a substantial nuclear suppression for negative hadrons produced with high  $p_T$  at large pseudorapidity  $\eta = 3.2$ , instead of the usual enhancement (see later in Fig. 3). Since the data cover rather small  $x_2 \sim 10^{-3}$ , it is tempting to interpret the suppression as either a result of saturation [15,16] or the color glass condensate [17], expected in some models [18].

Note, however, that the data span a region of rather large  $x_F$ , where all known reactions, both hard and soft, show considerable nuclear suppression. Moreover, available data indicate that this effect scales with  $x_F$  rather than with  $x_2$  as one would expect if the scaling were the net effect of coherence.

Indeed, the collection [19–21] of data depicted in Fig. 2 for the production of different species of hadrons in  $pA$

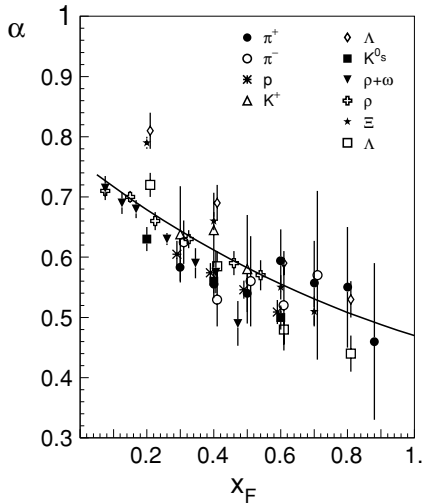


FIG. 2. Exponent describing the  $A$  dependence ( $\propto A^\alpha$ ) of the ratio for the production of different hadrons in  $p$ -Au relative to  $pp$  collisions as function of  $x_F$ . Collection of data and references can be found in [19–21]. Curve is result of a parameter-free calculation using Eq. (11).

collisions at different energies, with the nuclear dependence parametrized as  $A^\alpha$ , exhibit universality and  $x_F$  scaling.

Data from the E866 experiment at Fermilab for nuclear effects in  $J/\Psi$  and  $\Psi'$  production [22], shown later in Fig. 8, also exhibit a strong suppression that is seen to scale in  $x_F$  compared to lower-energy data [23] and that appears universal when compared with  $\Psi'$  [22]. Recent measurements of nuclear effects for  $J/\Psi$  production in D-Au collisions by the PHENIX Collaboration [24] at RHIC are consistent with  $x_F$  scaling, but they exhibit a dramatic violation of  $x_2$  scaling when compared with the E866 data [22].

The DY reaction is also known to be considerably suppressed at large  $x_F$  [2], as one can see later in Fig. 6. Unfortunately, no data sufficiently accurate to test  $x_F$  scaling are available at other energies.

There is a feature common to all these reactions; namely, when the final particle is produced with  $x_F \rightarrow 1$ , insufficient energy is left to produce anything else. As a class, such events are usually called large rapidity gap processes. Obviously, the restriction of energy conservation may cause substantial suppression. This is analogous to what happens in QED when elastic electron scattering occurs with no bremsstrahlung within a given resolution; it is described by what is known as the Sudakov form factor. The LRG cross section is more strongly suppressed as the resolution improves.

If a large- $x_F$  particle is produced, the rapidity interval to be kept empty is  $\Delta y = -\ln(1 - x_F)$ . We describe particle production via perturbative gluon radiation [25] with subsequent nonperturbative hadronization. Assuming as usual an uncorrelated Poisson distribution for gluons, the Sudakov suppression factor, i.e., the probability to have a rapidity gap  $\Delta y$ , becomes

$$S(\Delta y) = e^{-(n_G(\Delta y))}, \quad (5)$$

where in our case  $n_G(\Delta y)$  is the mean number of gluons that would be radiated within  $\Delta y$  if energy conservation were not an issue.

Note that even in the case where no gluon is radiated within the rapidity gap, the hadronization can easily fill the gap with particles. The probability that this does not happen is another suppression factor which, however, is independent of target and cancels in the nucleus-to-proton ratio.

The mean number  $\langle n_G(\Delta y) \rangle$  of gluons radiated in the rapidity interval  $\Delta y$  is related to the height of the plateau in the gluon spectrum,  $\langle n_G(\Delta y) \rangle = \Delta y dn_G/dy$ . Then, the Sudakov factor acquires the simple form,

$$S(x_F) = (1 - x_F)^{dn_G/dy}. \quad (6)$$

The height of the gluon plateau was estimated by Gunion and Bertsch [25] as

$$\frac{dn_G}{dy} = \frac{3\alpha_s}{\pi} \ln \left( \frac{m_\rho^2}{\Lambda_{\text{QCD}}^2} \right). \quad (7)$$

The value of  $\alpha_s$  was fitted [25] to data on pion multiplicity in  $e^+e^-$  annihilation, where it was found that  $\alpha_s = 0.45$ . This is close to the critical value  $\alpha_s = \alpha_c = 0.43$  [26] and to the value  $\langle \alpha_s \rangle = 0.38$  calculated within a model of small gluonic spots when averaged over the gluon radiation spectrum [27]. For further calculations, we take  $\alpha_s = 0.4$ , which gives with high accuracy  $dn_G/dy = 1$ , i.e., the Sudakov factor,

$$S(x_F) = 1 - x_F. \quad (8)$$

Amazingly, this coincides with the suppression factor applied to every additional Pomeron exchange in the quark-gluon string [28] and dual parton [29] models based on the Regge approach.

Clearly, on a nuclear target, the Sudakov suppression factor should fall more steeply as  $x_F \rightarrow 1$  since multiple interactions enhance the transverse kick given to the projectile parton and therefore tend to shake off (i.e., to radiate) more gluons. This can be understood in terms of the Fock state decomposition. Specifically, according to the counting rules [4], the behavior of the single-parton distribution function for  $x_1 \rightarrow 1$  depends on the number of constituents in the particular Fock state. A nucleus having a higher resolution, controlled by the saturation scale  $Q_s$  [16,17], resolves more constituents and thus results in a steeper fall off of the distribution function toward  $x_1 = 1$ .

We come to the nontrivial conclusion that the effective parton distribution function in the beam hadron depends on the target. Such a process dependence constitutes an apparent breakdown of QCD factorization and is a leading twist effect.

One can also formulate this suppression as  $x_F \rightarrow 1$  as a survival probability of the LRG in multiple interactions with the nucleus. Clearly, every additional inelastic interaction contributes an extra suppression factor  $S(x_F)$ . The probability of an  $n$ -fold inelastic collision is related to the Glauber model coefficients via the Abramovsky-Gribov-Kancheli (AGK) cutting rules [30]. Correspondingly, the survival probability

at impact parameter  $\vec{b}$  reads

$$W_{\text{LRG}}^{hA}(b) = \exp \left[ -\sigma_{\text{in}}^{hN} T_A(b) \sum_{n=1}^A \frac{1}{n!} \left[ \sigma_{\text{in}}^{hN} T_A(b) S(x_F) \right]^n \right]. \quad (9)$$

In this expression, particles (gluons) are assumed to be produced independently in multiple rescattering, i.e., in Bethe-Heitler regime. Of course, it should be corrected for effects of coherence which turn out to be either small or absent, i.e., they can be neglected. Indeed, at small  $x_F$ , the Sudakov factor  $S(x_F \rightarrow 0) \rightarrow 1$ , and Eq. (9) takes the form of the standard Glauber expression for absorptive hadron-nucleus cross section. In this case, the coherence effects are known as Gribov inelastic shadowing corrections which are known to be quite small, a few percent [31].

In another limiting case,  $x_F \rightarrow 1$  energy conservation allows only radiation of low-energy gluons having short coherence time. Therefore, particles are produced incoherently in multiple interactions, and Eq. (9) is legitimate.

At large  $x_F \sim 1$ , Eq. (9) is dominated by the first term; therefore, integrating over impact parameter, one gets for the nucleus-to-proton ratio,  $R_{A/p}(x_F \rightarrow 1) \sim A^{1/3}$ . This expectation is confirmed by a measurement [32] of the  $A$  dependence of the cross section for the LRG process  $pA \rightarrow pX$ , quasifree diffractive excitation of the nucleus. The single diffraction cross section was found to be

$$\sigma_{\text{diff}}^{pA} = \int_{0.925}^1 dx_F \frac{d\sigma(pA \rightarrow pX)}{dx_F} = \sigma_0 A^\alpha, \quad (10)$$

with  $\alpha = 0.34 \pm 0.02$ , consistent with the above expectation.

#### IV. PRODUCTION OF LEADING HADRONS WITH SMALL $p_T$

The collection of data from [19–21] for the production of different species of particles in  $pA$  collisions, depicted in Fig. 2, exhibits quite strong and universal nuclear suppression at large  $x_F$ . Moreover, these data spanning the laboratory energy range from 70 to 400 GeV demonstrate that the nuclear effects scale in  $x_F$ .

It is natural to relate the observed suppression to the dynamics discussed above, which is close to the description of soft inclusive reactions within the quark-gluon string [28], or dual parton [29] models.

The nuclear effects can be calculated summing over  $n$  and integrating over the impact parameter in Eq. (9),

$$R_{A/N}(x_F) = \frac{1}{(1-x_F)\sigma_{\text{abs}}A} \int d^2b e^{-\sigma_{\text{abs}}T_A(b)} \times [e^{(1-x_F)\sigma_{\text{abs}}T_A(b)} - 1]. \quad (11)$$

In the Glauber model, the effective cross section is the familiar inelastic  $NN$  scattering cross section. However, the actual number of collisions, which determines the value of the effective absorption cross section, is subject to considerable modification from Gribov's inelastic shadowing corrections, which make the nuclear medium substantially more transparent. These corrections considerably reduce both the num-

ber of collisions and the effective absorption cross section  $\sigma_{\text{abs}}$  [31,33].

To compare with data, the nuclear effects are parametrized as  $R_{A/N} \propto A^\alpha$ , where  $\alpha$  varies with  $A$ . We use  $A = 40$ , for which the Gribov corrections evaluated in [33] lead to an effective absorption cross section  $\sigma_{\text{abs}} \approx 20$  mb. Then the simple expression Eq. (11) explains the observed  $x_F$  scaling and describes rather well the data depicted in Fig. 2.

One may wonder why  $\alpha(x_F)$  plotted in Fig. 2 does not reach values as small as  $1/3$ , even when  $x_F \rightarrow 1$ . As mentioned, this exponent varies with  $A$ , and simple geometrical considerations may be accurate only for sufficiently heavy nuclei. In the case of diffraction [33], a specific enhancement of the effective absorption cross section makes  $\alpha$  smaller in this case, in good accord with data [32].

Note that our description is very close to that in the dual parton model (or quark-gluon string model) [34]. However, we present a different interpretation of the same phenomena and introduce Gribov corrections for inelastic shadowing, which substantially reduce the number of collisions.

#### V. HIGH- $p_T$ HADRON PRODUCTION AT FORWARD RAPIDITIES, THE BRAHMS DATA

The BRAHMS Collaboration measured nuclear effects for production of negative hadrons at pseudorapidity  $\eta = 3.2$  and transverse momentum up to  $p_T \approx 4$  GeV. Instead of the usual Cronin enhancement, a suppression was found, as one can see from Fig. 3.

First, consider the rather strong suppression of the data at small  $p_T$ . One can understand this in terms of the simple

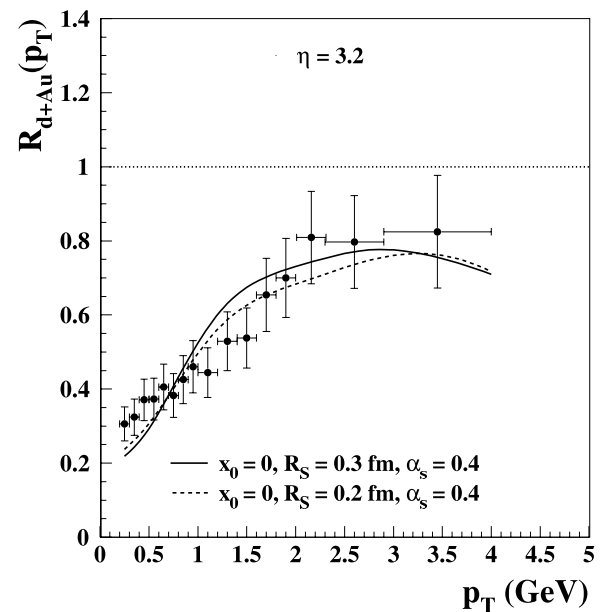


FIG. 3. Ratio of negative particle production rates in  $d$ -Au and  $pp$  collisions as function of  $p_T$ . Data are from [1], solid and dashed curves correspond to calculations with the diquark size 0.3 and 0.4 fm, respectively.

relation for the  $p_T$ -integrated cross sections,

$$\int d^2 p_T \frac{d\sigma}{d\eta d^2 p_T} = \left\langle \frac{dn}{d\eta} \right\rangle \sigma_{\text{in}}. \quad (12)$$

The mean number of produced particles per unit rapidity  $\langle dn/d\eta \rangle$  has an  $A$  dependence that varies with rapidity. Particle production at mean rapidity is related to the radiation of gluons, whose multiplicity rises as  $dn_G/d\eta \propto A^{1/3}$  (for the moment we neglect gluon shadowing and assume the Bethe-Heitler regime for gluon radiation). Since the inelastic cross section  $\sigma_{\text{in}}^{pA} \propto A^{2/3}$ , the integrated inclusive cross section, Eq. (12), rises linearly with  $A$ . This is in accordance with the AGK cancellation [30] of shadowing for the inclusive cross section known as the Kancheli-Mueller theorem.

Nuclei modify the  $p_T$  distribution of radiated gluons, an effect known as the color glass condensate (CGC) [16,17] or Cronin effect [35,36]. Due to this effect, gluons are suppressed at small  $p_T$ , enhanced at medium  $p_T$ , and unchanged at large  $p_T$ . Gluon shadowing, or the Landau-Pomeranchuk effect, is part of the CGC and reduces the total number of radiated gluons more strongly at small than at large  $p_T$ . Thus, the observed strong suppression of small- $p_T$  particle production at midrapidities is a manifestation of the CGC.

One, however, should be careful with the interpretation of data in terms of the CGC, which is supposed to be a result of coherence between different parts of the nucleus. It turns out that nuclear modifications of the transverse momentum distribution occur in both the coherent and incoherent regimes. While the former can be an effect of the CGC, the latter has little to do with this phenomenon. In particular, the RHIC data at midrapidities are in the transition region, i.e., particles are produced coherently on the nucleus at small  $p_T \lesssim 1$  GeV, but incoherently at larger  $p_T$  [36].

The suppression at small  $p_T$  observed at  $\eta = 3.2$  is even stronger than at midrapidities. At this rapidity, the overall scale of the suppression is related to the fact that particle production is dominated by fragmentation of the projectile valence quarks. Gluons are additionally suppressed due to softness of the gluon fragmentation function leading to a substantially larger value of  $x_1$  for gluons than for pions. Therefore, the origin of the suppression is quite different from that at midrapidity [37]. Because the number of valence quarks is fixed and equal to 3 when integrated over rapidity (Gottfried sum rule), the number of valence quarks produced with  $x_F \rightarrow 1$  must be even smaller, and accordingly the ratio of the  $p_T$ -integrated inclusive cross sections should be suppressed well below unity. In this case, we can use either our results or the data plotted in Fig. 2, both of which suggest a suppression factor of approximately  $A^{-0.3} \approx 0.2$ , in good agreement with the BRAHMS data. This suppression is not affected by either the CGC or gluon shadowing.

Note that the dominance of valence quarks in the projectile proton leads to an isospin-biased ratio. Namely, negative hadrons with large  $p_T$  close to the kinematic limit are produced mainly from  $u$ , rather than  $d$ , quarks. Therefore, more negative hadrons are produced by deuterons than by protons, and this causes an enhancement of the ratio plotted in Fig. 3 by a factor

of 3/2 [37]. Further on, we take care of this by using proper fragmentation functions for negative hadrons.

The cross section of hadron production in  $dA(pp)$  collisions is given by a convolution of the distribution function for the projectile valence quark with the quark scattering cross section and the fragmentation function,

$$\frac{d\sigma}{d^2 p_T d\eta} = \sum_q \int_{z_{\text{min}}}^1 dz f_{q/d(p)}(x_1, q_T^2) \times \frac{d\sigma[qA(p)]}{d^2 q_T d\eta} \Big|_{\vec{q}_T = \vec{p}_T/z} D_{h^-/q}(z). \quad (13)$$

Here,

$$x_1 = \frac{q_T}{\sqrt{s}} e^\eta. \quad (14)$$

We use the lowest order parametrization of Gluck, Reya, and Vogt [38] for the quark distribution in the nucleon. As explained above, the interaction with a nuclear target does not obey factorization, since the effective projectile quark distribution correlates with the target. Summed over multiple interactions, the quark distribution in the nucleon reads

$$f_{q/N}^{(A)}(x_1, q_T^2) = C f_{q/N}(x_1, q_T^2) \times \frac{\int d^2 b [e^{-x_1 \sigma_{\text{eff}} T_A(b)} - e^{-\sigma_{\text{eff}} T_A(b)}]}{(1-x_1) \int d^2 b [1 - e^{-\sigma_{\text{eff}} T_A(b)}]}. \quad (15)$$

Here the normalization factor  $C$  is fixed by the Gottfried sum rule.

The cross section of quark scattering on the target in Eq. (13) is calculated in the light-cone dipole approach [39,40], which provides an easy way to incorporate multiple interactions. Obviously, the  $p_T$  distribution of hadrons in the final state is affected by the primordial transverse motion of the projectile quarks. In our calculation, we separate the contributions characterized by different initial transverse momenta and sum over three different mechanisms of high- $p_T$  production.

### A. Quark-diquark break up of the proton

We employ the quark-diquark model of the proton with a  $\widehat{u\bar{d}}$  diquark that is small compared to the proton radius [6,41]. Correspondingly, the third valence quark external to the diquark has much smaller transverse momentum than the two others sitting inside the diquark. As a first mechanism, we consider proton breakup  $p \rightarrow \widehat{q\bar{q}} + q$ . We treat the diquark  $\{qq\}$  as pointlike and integrate over its momentum. Then the  $k_T$  distribution of the projectile valence quark, after propagation through the nucleus at impact parameter  $\vec{b}$ , is given by [42,43]

$$\frac{d\sigma(NA \rightarrow qX)}{d^2 k_T d^2 b} = \int \frac{d^2 r_1 d^2 r_2}{(2\pi)^2} e^{i\vec{k}_T(\vec{r}_1 - \vec{r}_2)} \times \Psi_N^\dagger(r_1) \Psi_N(r_2) [1 + e^{-\frac{1}{2}\sigma_{q\bar{q}}^N(\vec{r}_1 - \vec{r}_2)T_A(b)} - e^{-\frac{1}{2}\sigma_{q\bar{q}}^N(\vec{r}_1)T_A(b)} - e^{-\frac{1}{2}\sigma_{q\bar{q}}^N(\vec{r}_2)T_A(b)}]. \quad (16)$$

Here the quark-diquark wave function of the nucleon is taken in a form that matches the known perturbative QCD behavior at large transverse momenta,  $\Psi_N(r) \propto K_0(r/R_p)$ , where  $K_0$

is the modified Bessel function,  $R_p^2 = \frac{4}{3}r_{\text{ch}}^2$ , and  $r_{\text{ch}}$  is the mean charge radius of the proton. We assume that the quark's longitudinal momentum dependence factorizes and is included in  $f_{q/N}(x_1)$ . The dipole cross section  $\sigma_{\bar{q}q}^N(r)$  is taken in the saturated form [43], inspired by the popular parametrization of Ref. [44], but adjusted to the description of soft data.

This contribution dominates the low transverse momentum region  $k_T \lesssim 1$  GeV.

### B. Diquark break up $\widehat{q\bar{q}} \rightarrow qq$

At larger  $k_T$ , the interaction resolves the diquark, so its break-up should be considered. This contribution is calculated in accordance with Refs. [42,43],

$$\begin{aligned} \frac{d\sigma(\widehat{q\bar{q}}A \rightarrow qX)}{d^2k_T d^2b} &= \int \frac{d^2r_1 d^2r_2}{2(2\pi)^2} e^{i\vec{k}_T(\vec{r}_1 - \vec{r}_2)} \\ &\times \Psi_D^\dagger(r_1) \Psi_D(r_2) \left[ 2 - e^{-\frac{1}{2}\sigma_{\bar{q}q}^N(\vec{r}_1)T_A(b)} \right. \\ &- e^{-\frac{1}{2}\sigma_{\bar{q}q}^N(\vec{r}_2)T_A(b)} - e^{-\frac{1}{2}\sigma_{\bar{q}q}^N(\vec{r}_2/2)T_A(b)} \\ &- e^{-\frac{1}{2}\sigma_{\bar{q}q}^N(\vec{r}_2/2)T_A(b)} - e^{-\frac{1}{2}\sigma_{\bar{q}q}^N(\vec{r}_1 - \frac{1}{2}\vec{r}_2)} \\ &- e^{-\frac{1}{2}\sigma_{\bar{q}q}^N(\vec{r}_2 - \frac{1}{2}\vec{r}_1)} + 2e^{-\frac{1}{2}\sigma_{\bar{q}q}^N(\vec{r}_1 - \vec{r}_2)T_A(b)} \\ &\left. + 2e^{-\frac{1}{2}\sigma_{\bar{q}q}^N(\frac{\vec{r}_1 - \vec{r}_2}{2})T_A(b)} \right]. \quad (17) \end{aligned}$$

The diquark wave function is also assumed to have a Bessel function form, with a mean quark separation of 0.2–0.3 fm. There is much evidence that such a small diquark represents the dominant quark configuration in the proton [41].

### C. Hard gluon radiation $q \rightarrow Gq$

At large  $k_T$ , the dipole approach should recover the parton model [45], where high momentum transfer processes occur (in leading order) as binary collisions with the transverse momentum of each final parton of order  $k_T$ . Clearly, this is different from the description in Eqs. (16) and (17), where one assumes that the projectile valence quark acquires high transverse momentum as a result of multiple rescatterings, while the radiated gluons that balance this momentum are summed to build up the dipole cross section. The latter is fitted to DIS data involving gluons of rather low transverse momenta. Therefore, one should explicitly include in the dipole description radiation of a gluon with large transverse momentum that approximately balances  $k_T$ , i.e., the process  $qN \rightarrow qGX$ . In the dipole approach, the cross section is given by the same formula, Eq. (16), except that the nucleon wave function is replaced by the quark-gluon light-cone wave function,  $\Psi_N(r_T) \Rightarrow \Psi_{qG}(r_T)$  [42,46], where [43]

$$\Psi_{qG}(\vec{r}_T) = -\frac{2i}{\pi} \sqrt{\frac{\alpha_s}{3}} \frac{\vec{r}_T \cdot \vec{e}^*}{r_T^2} \exp\left(-\frac{r_T^2}{2r_0^2}\right) \quad (18)$$

and  $r_0 = 0.3$  fm. Such a small mean quark-gluon separation is a result of a phenomenological analysis of data for soft single diffraction  $pp \rightarrow pX$ . The only way to explain the abnormally small triple-Pomeron coupling, which is translated into very weak diffractive gluon radiation, is to assume that the Weizsäcker-Williams gluons in the proton are located within

small spots [47]. The spot size  $r_0$  was fitted to diffractive data [43], and the result  $r_0 = 0.3$  fm agrees with both lattice calculations [48] and the phenomenological model of the instanton liquid [49].

Notice that at small  $k_T$  there is a risk of double counting in such a procedure, since the radiated gluon may be counted twice, explicitly and implicitly as a part of the dipole cross section. However, the first two contributions, Eqs. (16) and (17), and the last one dominate in different regions of  $k_T$ , and we found their overlap to be very small.

### D. Gluon shadowing

Although the BRAHMS data involve rather large values of  $x_F$ , the corresponding values of  $x_2$  are so small that the considerations of Secs. II and VII lead to little reduction of the coherence length. Nevertheless, gluon shadowing corrections are expected to be quite small even at very small  $x_2$ ; e.g., see predictions for Large Hadron Collider (LHC) in Ref. [36]. This is related to the presence of small-size gluonic spots in nucleons, discussed in the previous Sec. V C. Indeed, one goes to small  $x_2$  to make the coherence length longer ( $l_c \propto 1/x_2$ ) and thus to arrange an overlap between the parton clouds which belong to different nucleons separated in the longitudinal direction. However, even if this condition is fulfilled, the gluon clouds hardly overlap in impact parameter if they are shaped as small-size spots. Expecting the strongest gluon shadowing at  $Q^2 \rightarrow 0$ , one can estimate the shadowing correction to be

$$R_G(b) \sim 1 - \exp\left[-\frac{3\pi}{4} r_0^2 T_A(b)\right]. \quad (19)$$

For heavy nuclei, this estimate gives a rather weak shadowing of about 10%, in good accord with more accurate calculations [43,50] or with the next-to-leading order analysis of nuclear DIS data [51].

We calculate gluon shadowing corrections within the dipole approach with the light-cone gluon distribution function, Eq. (18); the details can be found in [43,50].

### E. Comparison with data

First of all, one should confront the model with the  $p_T$ -dependent cross section of hadron production in  $pp$  collisions. Although the nuclear effects under discussion are not sensitive to this dependence, which mostly cancels in the  $dA/pp$  ratio, this would be a stringent test of the model. Our calculations are compared with  $pp$  data from the BRAHMS experiment at  $\eta = 3.2$  in Fig. 4. In view of the isospin asymmetry of leading particle production mentioned above, it is important to use proper fragmentation functions. The standard ones extracted from data on  $e^+e^-$  annihilation give a sum of positive and negative hadrons, while one needs only fragmentation functions for production of negative hadrons in order to compare with the BRAHMS data. We use these negative fragmentation functions in our calculations [52].

Now we are in a position to predict nuclear effects employing the dipole formalism and the mechanism described above. The results are compared with the BRAHMS data for the minimum-bias ratio [1] in Fig. 3. One can see that

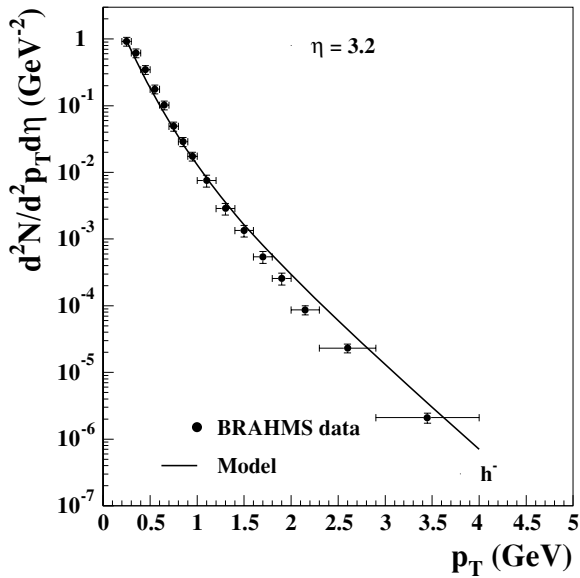


FIG. 4. Number of negative hadrons vs  $p_T$  produced in  $pp$  collisions at  $\sqrt{s} = 200$  GeV and pseudorapidity  $\eta = 3.2$ . Our calculations, given by the solid curve, are compared with BRAHMS data [1].

this parameter-free calculation does not leave much room for other mechanisms, including a strong CGC. On the other hand, our calculations do include the CGC via explicit gluon radiation and via gluon shadowing. This is, however, a rather moderate effect due to the smallness of the gluonic spots in nucleons [43,47,49], as described by the quark-gluon wave function in Eq. (18).

It is interesting also to check whether the predicted dependence of the ratio on impact parameter is supported by data. Our results for the ratio of the cross sections of central and semicentral to peripheral collisions are depicted in Fig. 5 in comparison with BRAHMS data [1]. The agreement is rather good.

Although the BRAHMS Collaboration has presented their results for nuclear effects as a function of rapidity, we skip this comparison, since it cannot fail. Indeed, predictions [36] for the Cronin effect at  $\eta = 0$  published in advance of data were quite successful. That region is dominated by production and fragmentation of gluons. The very forward region, which is under consideration now, is dominated by production and fragmentation of valence quarks, and our calculations are successful here as well. For these reasons, we should not be much off the data at any other (positive) rapidity, which differs only in the relative contributions of valence quarks and gluons.

**VI. NUCLEAR SUPPRESSION OF DILEPTONS AT LARGE  $x_F$**

The E772 experiment at Fermilab [53] first observed that the DY process is suppressed at large  $x_F$ . Two mechanisms that may possibly be responsible for this effect have been considered so far: energy loss in the initial state [2,54,55] and shadowing [2,53]. To make the interpretation more certain and

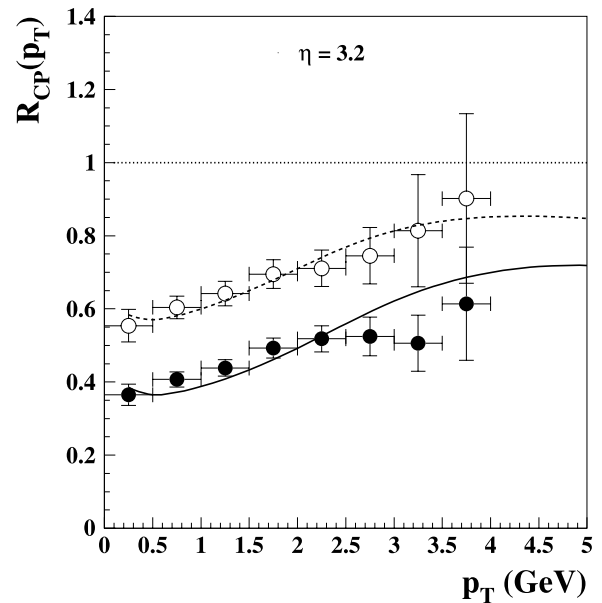


FIG. 5. Ratio of negative particle production in central (0–20%) and semicentral (30–50%) to peripheral (60–80%)  $d$ -Au collisions, shown by closed and open points, respectively. Results of corresponding calculations are depicted by solid and dashed curves.

to disentangle these two options, one can select data with the dilepton effective mass sufficiently large to ensure that the coherence length is too short for shadowing. An example of such data for the ratio of tungsten to deuterium is depicted in Fig. 6.

**A. Rest frame description**

According to the rest frame interpretation [14] (see also [42,56–59]), the DY process looks like fragmentation of a projectile quark into a dilepton via bremsstrahlung of a heavy photon. One can either calculate this perturbatively and use the quark distribution function at the corresponding scale or employ the soft quark distribution functions and use a phenomenological fragmentation function  $q \rightarrow q\bar{l}$ . The latter

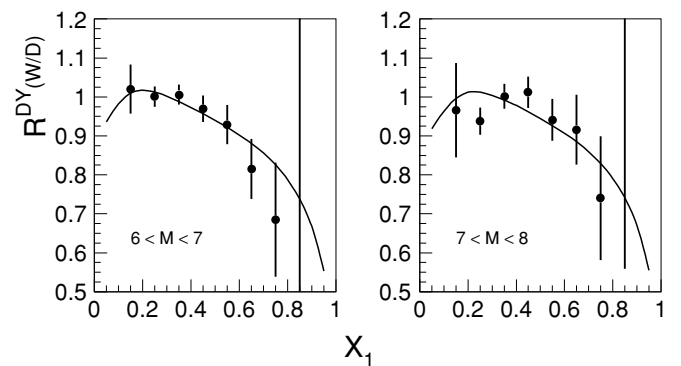


FIG. 6. Ratio of DY cross sections on tungsten and deuterium as a function of  $x_1$ , at large dilepton masses to eliminate nuclear shadowing.

approach, already used in [2], is appropriate here, and we will apply it using the cross sections of soft production of valence quarks in  $pp$  and  $pA$  collisions fitted in the following section. To the extent that these cross sections are subject to nuclear suppression at large  $x_F$ , the DY process should be suppressed as well.

We perform calculations within the same formalism used in [2], but the source of suppression is not a simple initial state energy loss, but an effective one that results from the nuclear modification of the Fock state decomposition discussed above. The nucleus-to-deuterium ratio reads

$$R_{A/D}(x_1) = \frac{2 \int_{x_1}^1 dx \frac{d\sigma(pA \rightarrow qX)}{dx} D_{\bar{l}/q}\left(\frac{x_1}{x}\right)}{A \int_{x_1}^1 dx \frac{d\sigma(pD \rightarrow qX)}{dx} D_{\bar{l}/q}\left(\frac{x_1}{x}\right)}. \quad (20)$$

Here we implicitly take into account the difference in the isospin composition of deuterium and tungsten. We also incorporate the contribution of projectile antiquarks and target quarks using the CETQ Collaboration's quark distribution functions [60].

### B. Nuclear suppression of valence quarks

To evaluate Eq. (20), one needs to know the cross sections of soft valence quark production in  $pp$  and  $pA$  collisions. To obtain this, we turn the problem around, trying to be more model independent, and get the nuclear suppression of valence quark jets directly from data. For this purpose, we fitted data [19] for pion production in  $pp$  and  $pA$  collisions at 100 GeV. We describe the spectrum of produced pions as

$$\frac{d\sigma(pA \rightarrow \pi X)}{dx_1} = \int_{x_1}^1 dx \frac{d\sigma(pA \rightarrow qX)}{dx} D_{\pi/q}(x/x_1). \quad (21)$$

The fragmentation function  $q \rightarrow \pi$ ,  $D_{\pi/q}(z)$ , is known. We use the form suggested by the Regge approach [28],  $D_{\pi^+/u} = D_{\pi^-/d} = (1-z)^{-\alpha_R+\lambda}$  and  $D_{\pi^+/d} = D_{\pi^-/u} = (1-z)D_{\pi^+/u}$ , where  $\lambda \approx 1/2$ .

The unknown function in Eq. (21) is the cross section for quark jet production in  $pp$  or  $pA$  collisions. We parametrized these cross sections by a simple  $x$  dependence,  $\propto (1-x^\epsilon)^u/\sqrt{x}$  and  $\propto (1-x^\epsilon)^d/\sqrt{x}$  for production of  $u$  and  $d$  quarks, respectively, performed a fit to Fermilab data [19] at 100 GeV, and found  $u = 1.85 \pm 0.07$ ,  $d = 3.05 \pm 0.15$  for  $pp$  collisions;  $u = 2.00 \pm 0.11$ ,  $d = 4.15 \pm 0.33$  for  $pA$  collisions; and  $u = 2.03 \pm 0.14$ ,  $d = 4.00 \pm 0.33$  for  $p$ -Pb collisions. The quality of the fit can be seen in Fig. 7.

While the parameter  $u$  does not show any strong  $A$  dependence, the value of  $d$  rises with  $A$  making the  $x$  dependence of the cross section steeper. This is no surprise, since  $d$  quarks have a steeper distribution function in the proton. Unfortunately, the data are not sufficient to fix well the parameter  $\epsilon$ , which is found to be  $\epsilon = 1.5 \pm 0.9$ .

### C. Comparison with data

Drell-Yan results based on Eq. (20) are compared with the E772 data in Fig. 6. For  $D_{\bar{l}/q}(z, M^2)$ , we used the phenomenological fragmentation function  $D_{\bar{l}/q}(z, M^2) \propto (1-z)^{0.3}$  that was fitted to data in Ref. [2] and found to be independent

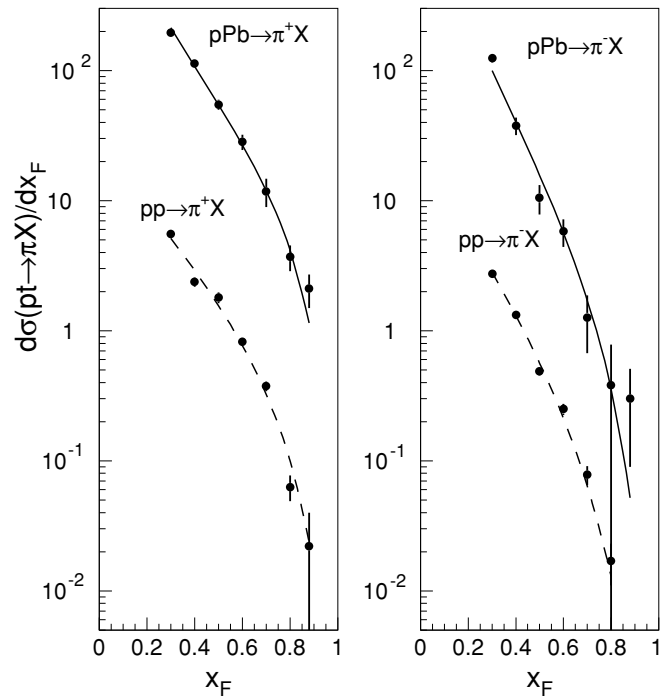


FIG. 7. Fit to data [19] for  $pp(A) \rightarrow \pi^\pm X$  with parametrization described in text. Results are shown by dashed and solid curves for  $pp$  and  $p$ -Pb collisions, respectively.

of the  $M^2$  within errors, and for the quark production cross sections we used the fit performed in the previous section. The parameter  $\epsilon$ , which is poorly defined by the data, affects the  $x_1$  dependence of the DY cross section ratio but hardly varies the amount of suppression at large  $x_F$ . We select  $\epsilon = 1.3$ , which is well within the errors and provides for  $R_{A/D}(x_1)$  a shape similar to the data.

Note that this description of nuclear effects appears different from the energy-loss scenario employed in [2]. There is, however, a strong overlap between the two mechanisms. The nuclear modification of the projectile Fock decomposition is just a different way of calculating nuclear effects due to gluon bremsstrahlung, which is the source of the induced energy loss. Therefore, the current approach might be called an effective energy-loss description. The results, however, are different. Namely, the simple mean energy loss of a single parton leads to nuclear modifications that scale in  $\Delta x_1$ , i.e., vanish with increasing energy at fixed  $x_1$ . In contrast, the current multiparton effective energy loss rises linearly with energy and leads to an  $x_1$  scaling in good accord with data.

Note that our interpretation of nuclear effects in the DY process is quite different from the description in [34], where nuclear effects are predicted to scale in  $x_2$  and are possible only if the coherence length is longer than the nuclear size. On the contrary, we expect the nuclear suppression to scale in  $x_F$ .

## VII. CHARMONIUM SUPPRESSION AT LARGE $x_F$

Nuclear suppression of charmonium production has been observed to be steeply increasing at large  $x_F \sim 1$  in many



experiments. Understanding this effect has been a challenge for a long time. Although the first data [23] were well explained and even predicted [61] by an energy-loss mechanism [54], later data on  $J/\Psi$  production at higher energies demonstrated that this mechanism is not sufficient, since it does not explain the observed  $x_F$  scaling.

This problem was studied within the dipole approach in [62]. A substantial part of the suppression was found to be a higher twist effect related to the large size of charmonia. Such a suppression is frequently identified with simple final-state absorption. However, at high energies, a  $\bar{c}c$  fluctuation of a projectile gluon propagates and attenuates through the entire nucleus [63–65]; moreover, in the case of hadroproduction, such a dipole is colored. A description of this process in terms of the light-cone dipole approach was developed in [62], and the cross section was calculated in a parameter-free way.

The rest of the suppression observed experimentally was prescribed to be the effect of energy loss and gluon shadowing. Within this interpretation of data, the observed  $x_1$  scaling looked like an accidental compensation of energy-loss corrections decreasing with energy and gluon shadowing effects rising with energy. Correspondingly, an approximate  $x_2$  scaling (broken at low energies by energy loss) was predicted in [62] for energies ranging between Fermilab (fixed targets) and RHIC. However, the recent data from the PHENIX experiment at RHIC found a dramatic violation of  $x_2$  scaling in strict contradiction with this prediction. In fact, any parton model based on QCD factorization predicts  $x_2$  scaling and contradicts these data.

We think that the higher twist nuclear shadowing was correctly calculated in [62], but that the gluon shadowing was miscalculated and led to the incorrect predictions for RHIC [62,66]. What was missed in [62] is the shrinkage of the coherence length toward the kinematic limit. This effect, found for the DY reaction in [2] and discussed above in Sec. II, is even more important for gluon shadowing. Due to proximity of the kinematic limit for  $J/\Psi$  production with  $x_F \rightarrow 1$ , the effective value of  $x_2$  is substantially increased,

$$\tilde{x}_2 \sim \frac{x_2}{1 - x_1}. \quad (22)$$

Additionally, the coherence length available for gluon shadowing gets another small factor  $P^G$ ,

$$l_c^G = \frac{P^G}{m_N \tilde{x}_2} = \frac{s P^G}{M_\Psi^2 m_N} x_1 (1 - x_1). \quad (23)$$

This factor was evaluated in [50] as  $P^G \approx 0.1$ . Thus, we conclude that for the kinematics of the E772/E866 experiments, the coherence length for gluon shadowing does not exceed  $l_c^G \lesssim 0.8$  fm, i.e., no gluon shadowing is possible. Therefore, one should search for an alternative explanation of the data.

Obviously, the same Sudakov effect that causes the large  $x_F$  suppression of other particles, in particular light hadrons and lepton pairs, affects the charmonium production as well. We can use the same results for nuclear softening of the produced valence quark, fitted to data, as for the DY reaction. Nevertheless, the phenomenological fragmentation function

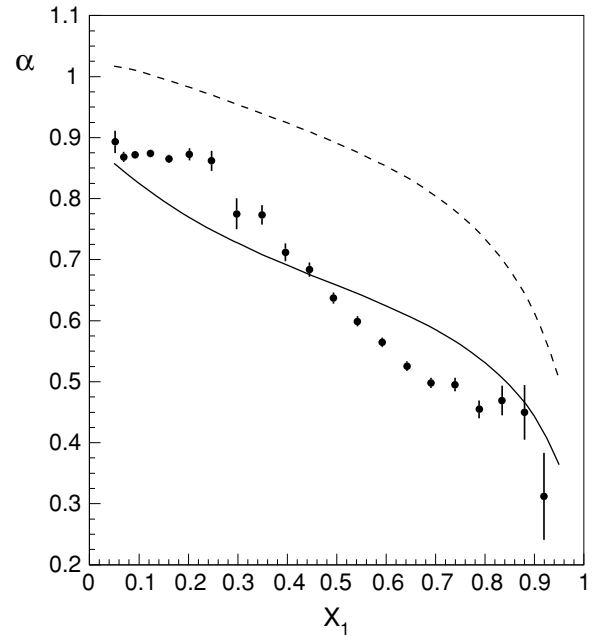


FIG. 8. Tungsten-to-beryllium cross section ratio for charmonium production as function of  $x_1$ . Data are from the E866 experiment [22]. Dashed curve shows the contribution of the extra Sudakov suppression extracted from data for soft hadron production. Solid curve also includes the higher twist shadowing related to the nonzero  $\bar{c}c$  separation.

$q \rightarrow \Psi q$  should be different. Fitting data for  $J/\Psi$  production in  $pp$  collisions, we found  $D_{\Psi/q}(z) \propto (1 - z)^{1.6}$ . Then, using the same convolution of the distribution function of the produced quark and the fragmentation function as in (20), we arrive at the suppression depicted by the dashed curve in Fig. 8.

After the higher twist shadowing calculated in [62] is added, the result is closer to the data, as shown by the solid curve in Fig. 8. We see that the scale of the nuclear suppression at large  $x_F$  agrees with the data, although the shape of the  $x_F$  dependence needs to be improved. This problem is a consequence of the oversimplified parametrization for the distribution function of the produced quark. Unfortunately, the errors of the available data for light hadron production are too large and do not allow the use of more sophisticated parametrizations.

Since the Sudakov suppression scales in  $x_1$ , one should expect an approximate  $x_F$  scaling, which is indeed observed in the data. Therefore, a similar  $x_F$  dependence is expected at RHIC and LHC, but the onset of  $x_2$  scaling, which has been naively expected at high energies [62], will never occur. Preliminary data from RHIC [24] confirm this. Additionally, they do not show any appreciable effect of gluon shadowing, in spite of the smallness of  $x_2$ . This agrees with the finding of [43], that the leading twist gluon shadowing is very weak. There is the possibility of a strong higher twist effect that may make gluon shadowing in the charmonium channel stronger than in DIS [62]. Such a prediction is based, however, on an *ad hoc* phenomenological potential model and may be incorrect.

Open charm production is expected to have a similar Sudakov nuclear suppression, as that shown by the dashed curve in Fig. 8. The higher twist shadowing related to the nonzero  $\bar{c}c$  separation does exist [67], but it is much weaker [67]. The leading twist gluon shadowing is also rather weak even at the RHIC energies. As for higher twist corrections, in the potential model [67] they may be large, but as we mentioned, this is not a solid theoretical prediction.

Note that our description of nuclear suppression of heavy quarkonia is quite different from the model proposed in [34]. That model involves three unknown parameters fitted to the nuclear data to be explained. The key parameter is the absorption cross section for a dipole consisting of a colored heavy quark pair  $\bar{Q}Q$  and light quarks. However, the pair of heavy quarks that eventually forms the detected quarkonium, and the comoving light quarks, cannot “talk to each other” due to Lorentz time dilation during propagation through the nucleus. In other words, it makes no difference whether the accompanying light quarks are primordial or created during hadronization of the color-octet  $\bar{Q}Q$  pair. Therefore, the multiple interactions of such a large dipole should not be treated as absorption for production of a colorless  $\bar{Q}Q$  pair via color neutralization. In contrast, in our approach the strong suppression of heavy quarks is related to the steep  $z$  dependence of the fragmentation function  $D_{\Psi/q}(z)$ . This function is fitted to data on  $pp$  collisions, while no fitting is done to nuclear data.

### VIII. CONCLUSIONS AND OUTLOOK

Nuclei suppress the large  $x_F$  production of different species of particles: light hadrons of both small and large  $p_T$ , dileptons, hidden and open heavy flavor, photons, etc. So far, no exception is known. The source of the effect can be understood either as an extra Sudakov suppression caused by multiple interactions in nuclei or as a nucleus-induced reduction of the survival probability of large rapidity gap processes. Although this effect can be also represented as an effective energy loss, the former scales in  $x_F$ . This is different from a simple single-parton energy loss, which is energy independent and leads to an energy shift  $\Delta x_1 = \Delta E/E$  that vanishes with energy.

In addition to this key observation, the new results of this paper can be presented as follows.

- (1) The simple formula (11) based on Glauber-Gribov multiple interaction theory and the AGK cutting rules explains

quite well the universal  $x_F$  scaling observed in data for inclusive production of leading light hadrons with small  $p_T$ .

- (2) With the same input, we calculated high- $p_T$  hadron production at large  $x_F$  and found a substantial suppression. This parameter-free calculation agrees with recent measurements performed by the BRAHMS Collaboration at forward rapidities in deuteron-gold collisions at RHIC. Our simple explanation is based on just energy conservation; therefore, it could be implemented independently of the dynamics. On the other hand, it does not leave much room for other mechanisms under debate, such as the CGC. We expect a similar suppression at large  $p_T$  and large  $x_F$  at lower energies, where no effect of coherence is possible.
- (3) The Drell-Yan process, treated like heavy photon bremsstrahlung in the target rest frame, is also subject to a nuclear suppression at large  $x_F$  imposed by energy conservation restrictions. In this case, we made a model-dependent calculation and relied on a fit to data for soft production of light hadrons. Within experimental uncertainties of the available data, we described rather well the data for the DY reaction at large masses where an alternative explanation, nuclear shadowing, is excluded.
- (4) Charmonium production is different from DY only by a steeper fragmentation function  $q \rightarrow \Psi q$ , which we fitted to  $pp$  data, and by an additional contribution of higher twist shadowing related to the large size of the charmonium. We correctly reproduced the magnitude of nuclear suppression at large  $x_F$ , but the shape of the  $x_F$  dependence needs to be improved. This problem seems to be a result of our model-independent, but oversimplified, fit to soft hadronic data. We leave this improvement for future work, both for charmonium production and the DY process.

### ACKNOWLEDGMENTS

We are grateful to Stan Brodsky, Gerry Garvey, Jörg Hüfner, Alexey Kaidalov, Yuri Kovchegov, Mike Leitch, Genya Levin, Pat McGaughey, Hans-Jürgen Pirner, and Jörg Raufeisen for useful discussions and to Berndt Müller for pointing to typos. The work of J.N. has been supported by the Slovak Funding Agency, Grant No. 2/4063/24. Work was supported in part by Fondecyt (Chile) Grants 1030355, 1050519, and 1050589.

---

[1] I. Arsene *et al.* (BRAHMS Collaboration), *Phys. Rev. Lett.* **93**, 242303 (2004).  
 [2] M. B. Johnson *et al.*, *Phys. Rev. Lett.* **86**, 4483 (2001); M. B. Johnson, B. Z. Kopeliovich, I. K. Potashnikova, P. L. McGaughey, J. M. Moss, and J. Peng, *Phys. Rev. C* **65**, 025203 (2002).  
 [3] E. Gotsman, E. Levin, and U. Maor, *Phys. Rev. D* **60**, 094011 (1999).  
 [4] R. Blankenbecler and S. J. Brodsky, *Phys. Rev. D* **10**, 2973 (1974).

[5] S. J. Brodsky and G. R. Farrar, *Phys. Rev. Lett.* **31**, 1153 (1973).  
 [6] I. A. Schmidt and R. Blankenbecler, *Phys. Rev. D* **15**, 3321 (1977).  
 [7] F. Niedermayer, *Phys. Rev. D* **34**, 3494 (1986).  
 [8] S. J. Brodsky and P. Hoyer, *Phys. Lett.* **B298**, 165 (1993).  
 [9] R. Baier, Yu. L. Dokshitzer, A. H. Mueller, S. Peigne, and D. Schiff, *Nucl. Phys.* **B483**, 297 (1997); **B484**, 265 (1997).  
 [10] B. Z. Kopeliovich, J. Nemchik, and E. Predazzi, in *Proceedings of the Workshop on Future Physics at HERA*, edited by G. Ingelman, A. De Roeck, and R. Klanner, DESY 1995/1996,

- Vol. 2, p. 1038; in *Proceedings of the ELFE Summer School on Confinement Physics*, edited by S. D. Bass and P. A. M. Guichon (Editions Frontieres, Cambridge, 1995), p. 391.
- [11] B. Z. Kopeliovich, J. Nemchik, E. Predazzi, and A. Hayashigaki, *Nucl. Phys.* **A740**, 211 (2004).
- [12] P. Hoyer, M. Vanttinen, and U. Sukhatme, *Phys. Lett.* **B246**, 217 (1990).
- [13] J. C. Collins, D. E. Soper, and G. Sterman, *Nucl. Phys.* **B261**, 104 (1985); *Adv. Ser. Direct. High Energy Phys.* **5**, 1 (1988).
- [14] B. Z. Kopeliovich, in *Proceedings of Workshop "Dynamical Properties of Hadrons in Nuclear Matter," Hirschegg'2005*, edited by H. Veldmeier (GSI, Darmstadt, 1995), p. 102.
- [15] L. V. Gribov, E. M. Levin, and M. G. Ryskin, *Nucl. Phys.* **B188**, 555 (1981); *Phys. Rep.* **100**, 1 (1983).
- [16] A. H. Mueller, *Eur. Phys. J. A* **1**, 19 (1998).
- [17] L. McLerran and R. Venugopalan, *Phys. Rev. D* **49**, 2233 (1994); **49**, 3352 (1994).
- [18] D. Kharzeev, Y. V. Kovchegov, and K. Tuchin, *Phys. Lett.* **B599**, 23 (2004).
- [19] D. S. Barton *et al.*, *Phys. Rev. D* **27**, 2580 (1983).
- [20] W. M. Geist, *Nucl. Phys.* **A525**, 149c (1991).
- [21] D. S. Barton *et al.*, *Phys. Rev. D* **27**, 2580 (1983); A. Beretvas *et al.*, *ibid.* **34**, 53 (1986); M. Binkley *et al.*, *Phys. Rev. Lett.* **37**, 571 (1976); R. Bailey *et al.*, *Z. Phys. C* **22**, 125 (1984); P. Skubic *et al.*, *Phys. Rev. D* **18**, 3115 (1978).
- [22] M. J. Leitch *et al.* (E866 Collaboration), *Phys. Rev. Lett.* **84**, 3256 (2000).
- [23] J. Badier *et al.* (NA3 Collaboration), *Z. Phys. C* **20**, 101 (1983).
- [24] R. G. de Cassagnac, PHENIX Collaboration, *J. Phys. G* **30**, S1341 (2004).
- [25] J. F. Gunion and G. Bertsch, *Phys. Rev. D* **25**, 746 (1982).
- [26] V. N. Gribov, *Eur. Phys. J. C* **10**, 71 (1999).
- [27] B. Z. Kopeliovich, I. K. Potashnikova, B. Povh, and E. Predazzi, *Phys. Rev. Lett.* **85**, 507 (2000); *Phys. Rev. D* **63**, 054001 (2001).
- [28] A. B. Kaidalov, *JETP Lett.* **32**, 474 (1980); *Sov. J. Nucl. Phys.* **33**, 733 (1981); *Phys. Lett.* **B116**, 459 (1982).
- [29] A. Capella *et al.*, *Phys. Rep.* **236**, 225 (1994).
- [30] V. A. Abramovsky, V. N. Gribov, and O. V. Kancheli, *Sov. J. Nucl. Phys.* **18**, 308 (1974); *Yad. Fiz.* **18**, 595 (1973).
- [31] B. Z. Kopeliovich, *Phys. Rev. C* **68**, 044906 (2003).
- [32] T. Akesson *et al.*, *Z. Phys. C* **49**, 355 (1991).
- [33] B. Z. Kopeliovich, I. K. Potashnikova, and Ivan Schmidt, e-Print Archive:hep-ph/0508277.
- [34] K. Boreskov, A. Capella, A. Kaidalov, and J. Tran Thanh Van, *Phys. Rev. D* **47**, 919 (1993).
- [35] D. Antreasyan, J. W. Cronin, H. J. Frisch, M. J. Shochet, L. Kluberg, P. A. Piroué, and R. L. Sumner, *Phys. Rev. D* **19**, 764 (1979).
- [36] B. Z. Kopeliovich, J. Nemchik, A. Schäfer, and A. V. Tarasov, *Phys. Rev. Lett.* **88**, 232303 (2002).
- [37] B. Z. Kopeliovich, talk at the Workshop on High- $p_T$  Physics at RHIC, December 2–6, 2003.
- [38] M. Gluck, E. Reya, and A. Vogt, *Z. Phys. C* **67**, 433 (1995).
- [39] A. B. Zamolodchikov, B. Z. Kopeliovich, and L. I. Lapidus, *JETP Lett.* **33**, 595 (1981); *Pisma v Zh. Eksper. Teor. Fiz.* **33**, 612 (1981).
- [40] M. B. Johnson, B. Z. Kopeliovich, and A. V. Tarasov, *Phys. Rev. C* **63**, 035203 (2001).
- [41] M. Anselmino *et al.*, *Rev. Mod. Phys.* **65**, 1199 (1993).
- [42] B. Z. Kopeliovich, A. Schäfer, and A. V. Tarasov, *Phys. Rev. C* **59**, 1609 (1999).
- [43] B. Kopeliovich, A. Schäfer, and A. V. Tarasov, *Phys. Rev. D* **62**, 054022 (2000).
- [44] K. Golec-Biernat and M. Wüsthoff, *Phys. Rev. D* **59**, 014017 (1999).
- [45] R. P. Feynman, R. D. Field, and G. C. Fox, *Phys. Rev. D* **18**, 3320 (1978).
- [46] Yu. V. Kovchegov and A. H. Mueller, *Nucl. Phys.* **B529**, 451 (1998).
- [47] B. Z. Kopeliovich and B. Povh, *J. Phys. G* **30**, S999 (2004).
- [48] M. D'Elia, A. Di Giacomo, and E. Meggiolaro, *Phys. Lett.* **B408**, 315 (1997).
- [49] E. V. Shuryak and I. Zahed, *Phys. Rev. D* **69**, 014011 (2004).
- [50] B. Kopeliovich, J. Raufeisen, and A. Tarasov, *Phys. Rev. C* **62**, 035204 (2000).
- [51] D. de Florian and R. Sassot, *Phys. Rev. D* **69**, 074028 (2004).
- [52] S. Kretzer, E. Leader, and E. Christova, *Eur. Phys. J. C* **22**, 269 (2001).
- [53] D. M. Alde *et al.*, *Phys. Rev. Lett.* **64**, 2479 (1990).
- [54] B. Z. Kopeliovich and F. Niedermayer, JINR-E2-84-834, Dubna, 1984 (scanned in KEK library).
- [55] M. Vasiliev *et al.*, *Phys. Rev. Lett.* **83**, 2304 (1999).
- [56] S. J. Brodsky, A. Hebecker, and E. Quack, *Phys. Rev. D* **55**, 2584 (1997).
- [57] B. Z. Kopeliovich, J. Raufeisen, and A. V. Tarasov, *Phys. Lett.* **B503**, 91 (2001).
- [58] B. Z. Kopeliovich, J. Raufeisen, A. V. Tarasov, and M. B. Johnson, *Phys. Rev. C* **67**, 014903 (2003).
- [59] R. Baier, A. H. Mueller, and D. Schiff, *Nucl. Phys.* **A741**, 358 (2004).
- [60] J. Pumplin *et al.*, *J. High Energy Phys.* 07 (2002) 012.
- [61] S. Katsanevas *et al.* (E537 Collaboration), *Phys. Rev. Lett.* **60**, 2121 (1988).
- [62] B. Z. Kopeliovich, A. V. Tarasov, and J. Hüfner, *Nucl. Phys.* **A696**, 669 (2001).
- [63] B. Z. Kopeliovich and B. G. Zakharov, *Phys. Rev. D* **44**, 3466 (1991).
- [64] J. Hüfner and B. Z. Kopeliovich, *Phys. Lett.* **B403**, 128 (1997).
- [65] Yu. P. Ivanov, B. Z. Kopeliovich, A. V. Tarasov, and J. Hüfner, *Phys. Rev. C* **66**, 024903 (2002).
- [66] B. Z. Kopeliovich, A. Polleri, and J. Hüfner, *Phys. Rev. Lett.* **87**, 112302 (2001).
- [67] B. Z. Kopeliovich and A. V. Tarasov, *Nucl. Phys.* **A710**, 180 (2002).